Journal of Zhejiang University-SCIENCE B (Biomedicine & Biotechnology)
ISSN 1673-1581 (Print); ISSN 1862-1783 (Online)
www.zju.edu.cn/jzus; www.springerlink.com
E-mail: jzus@zju.edu.cn

Rapid odor perception in rat olfactory bulb by microelectrode array*

Jun ZHOU, Qi DONG, Liu-jing ZHUANG, Rong LI, Ping WANG†‡

(*Biosensor National Special Lab, Key Lab for Biomedical Engineering of Ministry of Education, Department of Biomedical Engineering, Zhejiang University, Hangzhou 310027, China*)

†E-mail: cnpwang@zju.edu.cn

Received Mar. 12, 2012; Revision accepted Aug. 1, 2012; Crosschecked Oct. 30, 2012

Abstract: Responses of 302 mitral/tufted (M/T) cells in the olfactory bulb were recorded from 42 anesthetized freely breathing rats using a 16-channel microwire electrode array. Saturated vapors of four pure chemicals, anisole, carvone, citral and isoamyl acetate were applied. After aligning spike trains to the initial phase of the inhalation after odor onset, the responses of M/T cells showed transient temporal features including excitatory and inhibitory patterns. Both odor-evoked patterns indicated that mammals recognize odors within a short respiration cycle after odor stimulus. Due to the small amount of information received from a single cell, we pooled results from all responsive M/T cells to study the ensemble activity. The firing rates of the cell ensembles were computed over 100 ms bins and population vectors were constructed. The high dimension vectors were condensed into three dimensions for visualization using principal component analysis. The trajectories of both excitatory and inhibitory cell ensembles displayed strong dynamics during odor stimulation. The distances among cluster centers were enlarged compared to those of the resting state. Thus, we presumed that pictures of odor information sent to higher brain regions were depicted and odor discrimination was completed within the first breathing cycle.

Key words: Rapid odor perception, Mitral/tufted cell, Multielectrode array, Odor trajectory
doi:10.1631/jzus.B1200073 **Document code:** A **CLC number:** Q81

1 Introduction

Olfactory systems of vertebrates and invertebrates have complex anatomical structures, which enable animals to distinguish quickly thousands of odorous compounds. Olfactory sensory neurons in the olfactory epithelium interact with odor molecules and change chemical signals into electrical signals. The signals are then transmitted to a relay station called the olfactory bulb (OB) in vertebrates or the antennal lobe (AL) in invertebrates (Wilson and Mainen, 2006). The structure retains the projection and olfactory sensory neurons expressing the same olfactory receptor gene converge their axons into the same glomerulus in the OB (Mombaerts, 1996; Feinstein and Mombaerts, 2004; Couto *et al*., 2005). The circuitry in both OBs and ALs extracts and optimizes the relevant odorant information. In mammals, the principal neurons in the OB, named mitral/tufted (M/T) cells, display odor-dependent discharge, and deliver odorant information to high brain regions (Chen *et al*., 2009; Restrepo *et al*., 2009). To study the odor-specific response of OBs, a 2-deoxyglucose method by optical imaging were used for visualization of OB glomeruli (Meister and Bonhoeffer, 2001; Bathellier *et al*., 2007), and microelectrodes were implanted in OBs for recording spike trains of M/T cells (Kay and Laurent, 1999; Friedrich and Laurent, 2001; Egana *et al*., 2005; Rinberg *et al*., 2006; Davison and Katz,

‡ Corresponding author
* Project (Nos. 30970765 and 81027003) supported by the National Natural Science Foundation of China

2007; Cury and Uchida, 2010).

Rapid discrimination of odors enables animals to explore their environment. Inhalation behavior acts as a sampling process and captures odor molecules in the nose. This behavior is composed of passive breathing around 1–2 Hz and active sniffing around 4–12 Hz. The odor-induced activity of M/T cells is modulated by the breathing rhythm (Chaput, 1986; Isaacson and Cang, 2003). A single sniff in human studies shows sufficient time resolution for accurate odor discrimination (Laing, 1986; Leon and Johnson, 2003). A similar study was implemented in rats using a two-alternative odor discrimination task (Uchida and Mainen, 2003). Without behavioral and memorial influence existing in awake animals, how fast is the odor differentiation process in a free-breathing state? What kind of odor stimulus profiles do M/T cells sketch to communicate with downstream brain structures?

Inspired by the finding of rapid odor recognition in human experiments, we investigated the odor perception speed during a passive breathing state in rats. In the present study, we recorded the responses of an M/T cell ensemble to four pure chemicals in anesthetized freely breathing rats using a multielectrode array. Stimulated by a short puff, odor perception occurred within the first breathing cycle.

2 Materials and methods

2.1 Electrode preparation

Microwire electrode arrays play an important role in multi-site recording experiments. In this study, signals were obtained by home-made 16-channel nichrome microwire electrode arrays. Several key steps in the fabrication of high-quality electrodes include arranging microwires (65 μm nichrome, 300–500 kΩ at 1 kHz, AM system, Washington, USA; No. 762000) into the desired configuration and soldering microwires to the pad of a printed circuit board. Fig. 1a shows a photo of the 16-channel microwire electrode array.

2.2 Surgery

Male Sprague-Dawley rats weighting from 180–280 g were anesthetized with an intraperitioneal injection of chloral hydrate (4 ml/kg) and maintained with supplemental doses delivered once every 2 h. Each animal's temperature was kept to ~37 °C throughout the experiment. A small window (1.5 cm×1.5 cm) above the dorsal surface of the OB in one hemisphere was exposed by a hand drill and the dura was removed. The 16-channel microwire electrode array was lowered vertically into the mitral cell layer with up to two-micron spatial resolution using an MO-10 oil hydraulic microelectrode propeller (Narishige Group, Japan). The desired layer was identified by its large extracellular spiking activity, about 200–300 μm below the surface, which corresponds to the average depth of the mitral cell layer (Buonviso *et al*., 2003; Bathellier *et al*., 2008). After insertion, blood in the implant site was washed away and the surface of the OB was rinsed with saline to prevent drying. All of the procedures in this study conformed to the regulations for the administration of affairs concerning experimental animals (1988) and were approved by the Zhejiang University Animal Care and Use Committee.

2.3 Odorant delivery

Stimulations were performed with four pure chemical odorants: anisole (10 mmol/L), citral (10 mmol/L), carvone (10 mmol/L), and isoamyl acetate (10 mmol/L). All of the odorants were stored in liquid phase in glass vials at 0 °C, and were brought to room temperature before experiments. The saturated vapors from the head space of the vials were delivered to freely breathing rats through a custom-made olfactometer (Fig. 1d). A computer-controlled micro-vacuum pump and an electromagnetic valve allowed a puff stimulus to be given off around 2 ml in 0.5 s. The stimulus port was positioned 1 cm from the rat's nose. One stimulation session involved puffing one of four odors to the nose for 0.5 s, followed by clean air for 60 s. The procedure was then repeated with another odor until all four odors had been applied.

2.4 Electrophysiology recording and spike sorting

Individual neurons were recorded extracellularly in anesthetized freely breathing rats. The data from electrodes were amplified (1800×) and band-pass filtered (0.1 Hz to 2.0 kHz). All data were digitized at 40 kHz using an OmniPlex system (Plexon Inc., Dallas, TX, USA). The animal's breath was simultaneously monitored throughout the experiment using

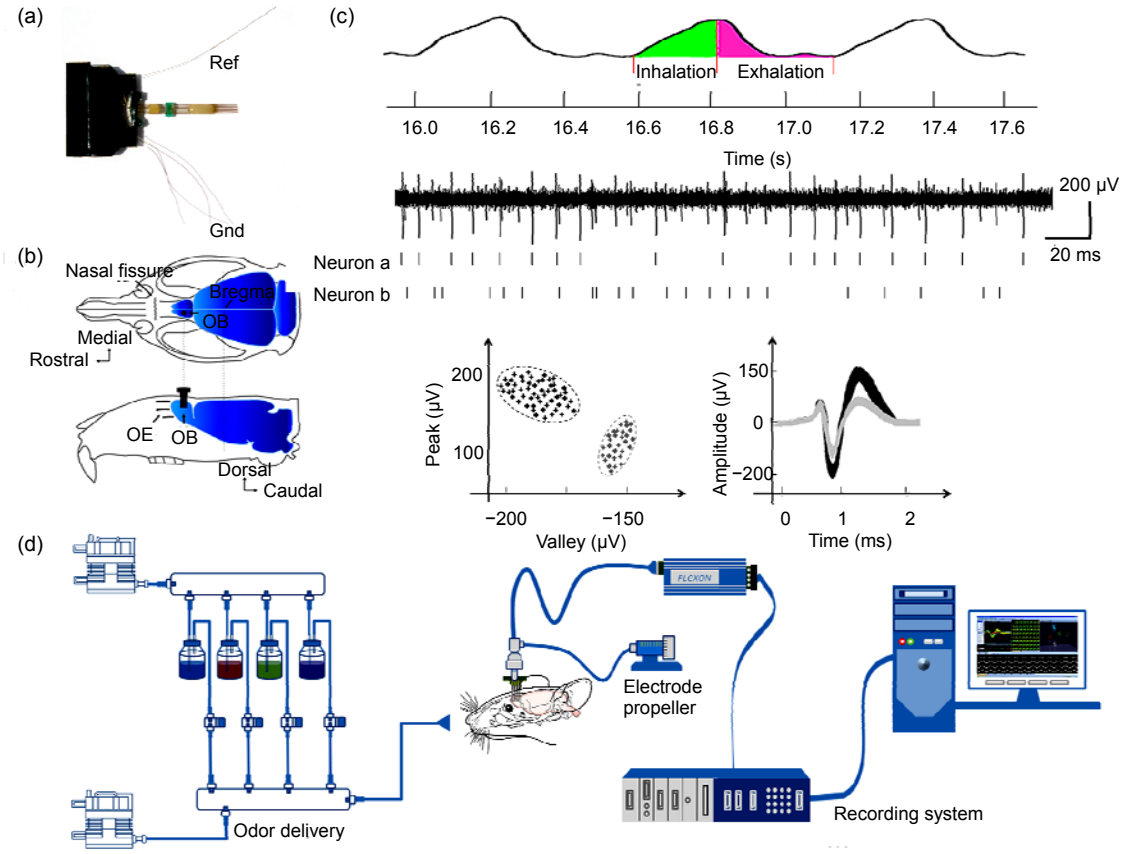

Fig. 1 Experimental system and extracellular recording of M/T cells

(a) A photo of the 16-channel microwire electrode array. Ref: reference; Gnd: ground. (b) The electrode array implanted in the dorsal surface of the OB in one hemisphere. OE: olfactory epithelium. (c) Upper panel: respiratory signal was recorded via a pressure sensor belt; lower panel: raw data after 200 Hz high-pass filtering and spike waveform segregation. (d) Experimental system including olfactometer, electrode propeller, and recording system. OB: olfactory bulb

each of the data dimensions. Then the covariance matrix of the vector was a piezoelectric respiratory sensor belt around the rat's chest. Fig. 1c (upper panel) shows a segment of recorded respiratory signal. Inhalation enlarged the volume of the chest and increased the pressure value from the baseline to the peak, while exhalation was indicated by the decline from the peak value to the baseline. On average, the time course of a breath was (580±8) ms with 240 ms inhalation and 340 ms exhalation. Most electrodes maintained a good signal-to-noise ratio during the experiments. Spike detection and identification was performed in offline sorter software (Plexon Inc.). Spikes were detected by a threshold on the 200 Hz high-pass filtered signals. The threshold was set at three sigma of the peak height. When multiple single units were detected by one electrode, their spike waveforms were separated by peak and trough amplitude, spike width, and other parameters. Fig. 1c (lower panel) shows an example of spike waveform segregation of two cells from one electrode.

2.5 Data analysis

All data analysis was performed using custom programs in MATLAB (MathWorks Inc., Massachusetts, USA). Spatiotemporal population analysis requires pooling results from all the responsive cells (Fig. 2b). To analyze the response of an M/T cell ensemble over time, we constructed a series of high dimensional vectors related to the four odor stimuli. Numbers of spikes were divided into successive, non-overlapping 100 ms bins. Each vector element consisted of the number of spikes in a single M/T cell during the time bin. Principal component analysis (PCA) was performed to characterize the response

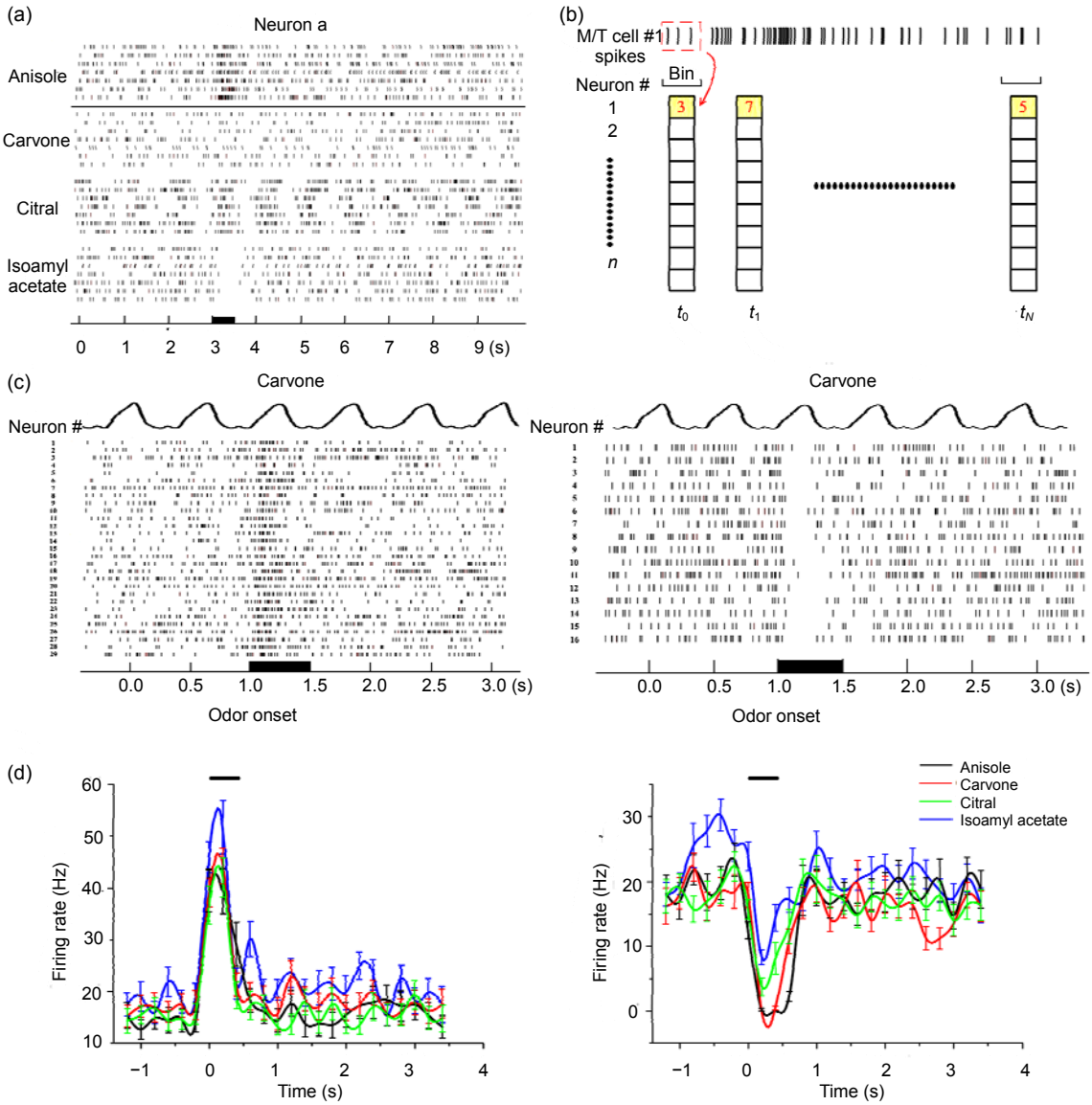

Fig. 2 Cell firing patterns and peristimulus-time histogram (PSTH)

(a) Representative single cell responses to four odors; (b) Formation of vectors that produce trajectories representing the evolution of the odor-evoked cell ensemble state; (c) Excitatory and inhibitory patterns of a cell ensemble responding to carvone; (d) Superimposed average PSTHs of excitatory (left) and inhibitory (right) M/T cells

trajectory by estimating a new set of points that satisfied dimensionality reduction with less information loss. First, the data in the vector was subtracted by the mean from acquired. After computing the eigenvectors and eigenvalues of the covariance matrix, three eigenvectors were selected to form a feature vector according to the first three highest eigenvalues. The transpose of the feature vector multiplied by the original data set provided the low dimension data for visualization of odor responses. For the plots in Fig. 3, principal components (PCs) were computed based on all activity vectors from 600 ms before to 1.2 s after odor onset. In Fig. 3b, the first three PCs contributed to between 64% and 87% of the total variance. In Fig. 3c, the captured variances of the first three PCs were 79%, 75%, 71%, and 74%. In Fig. 3d, the captured variances of the first three PCs were 72%, 83%, 77%, and 62%. To illustrate the odor classification of the OB, the responses of cell ensembles to four odors at the same time point was investigated. Vectors containing firing rates of 98 cells (72 excitatory and 26 inhibitory) at certain time points were constructed.

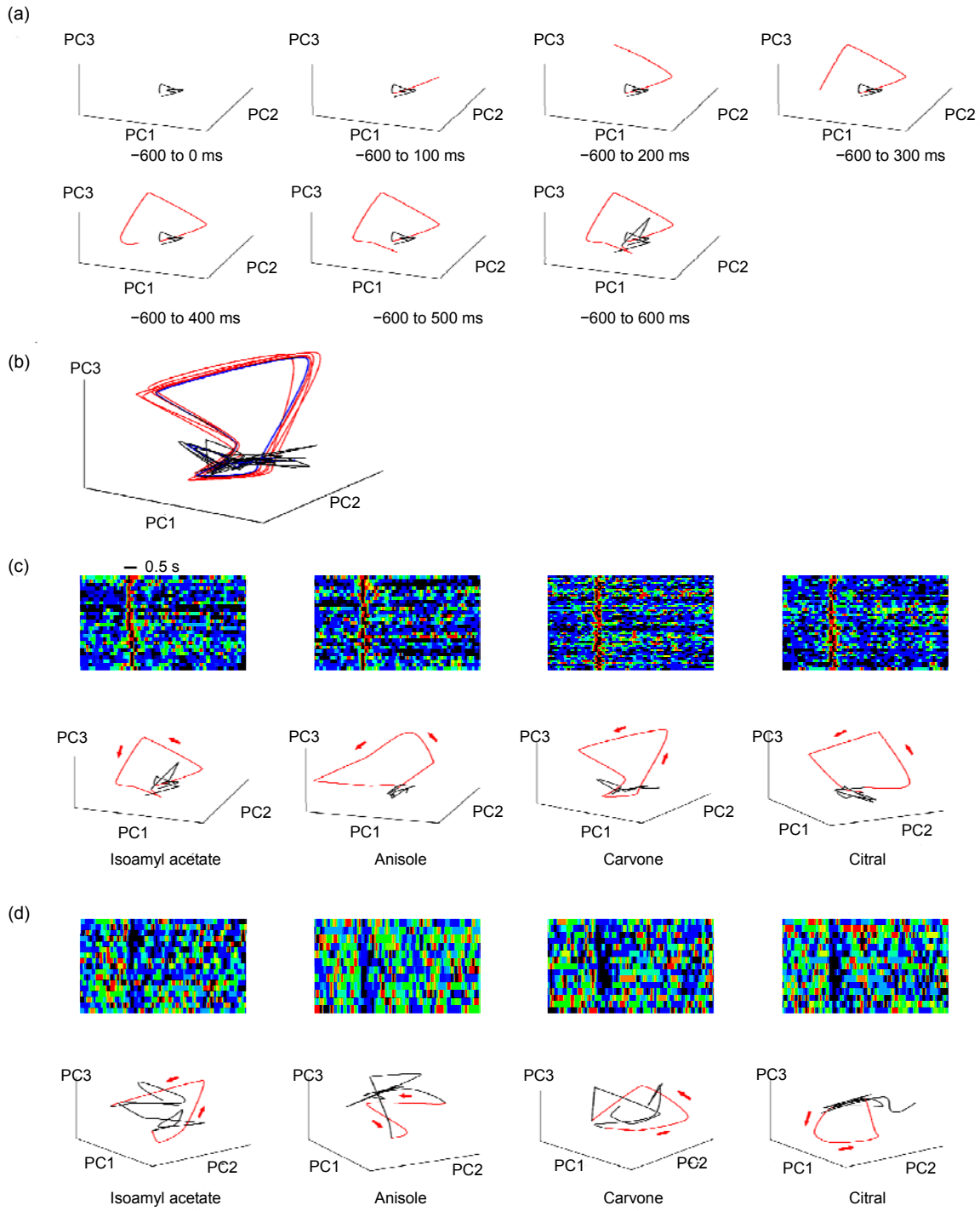

Fig. 3 Different temporal responses and trajectories of M/T cell ensemble activity evoked by different odors

(a) Evolution of the population response to isoamyl acetate with successive time points joined by a line. The red segment of the trajectory represents the epoch during the first breathing cycle after the odor stimulus. (b) Example of trial-to-trial variability. The trajectories for five trials in response to carvone, along with their mean (blue trace). (c) Excitatory temporal responses of four odors and corresponding trajectories averaged from five trials in their first three principal component (PC) axes. (d) Inhibitory temporal responses of four odors and corresponding trajectories averaged from five trials in their first three PC axes (Note: for interpretation of the references to color in this figure legend, the reader is referred to the web version of this article)

After applying PCA, the distances from odor cluster centers to the origin showed marked changes at three time points, i.e., 300 ms before odor onset, 100 ms after odor onset and 500 ms after odor onset. The sum of three PCs contained more than 90% of the total variance (Fig. 4).

We used a nonparametric test, the Kolmogorov-Smirnov test, to identify significant changes in firing rate during odor stimulation. The changes were represented by changes of spike distribution in a 580 ms window (the duration of one breathing cycle) after stimulation. The velocity was represented in the form of mean±standard deviation (SD) and the differences among odor-evoked cell ensemble trajectories were assessed using a one-way analysis of variance (ANOVA) test. The α value was set to 0.05 and we applied the Tukey's test for mean velocity comparisons.

3 Results and discussion

The activities of M/T cells were recorded from 42 anesthetized freely breathing rats. Spontaneous activities of cells represented independent responses and had widely variable firing rates (mean 11.4 spikes/s, range 0.8–18.2 spikes/s), similar to the results of Chaput *et al*. (1992). Odor cues strongly modulated the activities of M/T cells. In our recordings, a short odor puff (0.5 s) was delivered to the rat's nose and odor-evoked discharges occurred sequentially. Of all recording units perceiving four odor stimuli, 302 cells responded by exhibiting significantly modified spontaneous activity during the entire stimulus for at least one odor stimulus. The odor-evoked spike distribution in the 580 ms window after odor stimulation was significantly different from that of the blank control (p<0.05, Kolmogorov-Smirnov test). In about 60% of recordings, M/T cells were recorded that could not be activated by any of the stimuli used. These cells may be not selective for the tested odors. The observed temporal responses of cells were categorized into two types, excitatory patterns and inhibitory patterns (Fig. 2c), consistent with previous studies (Wellis *et al*., 1989; Davison and Katz, 2007). Fig. 2a shows typical responses of single M/T cells to different odors. Beyond excitatory and inhibitory responses, cells also showed sparse firing and firing modulated by respiration, which were considered as not responsive to odors. When the same odor stimulation session was repeated, these cell-odor pairs produced identical firing patterns. Among all responsive M/T cells, 9.3% cells responded to more than three odors, 23.2% cells responded to two odors and 67.5% cells responded to only one odor. The tendency of cells to be more easily activated by a single odor than by multiple odors implies that selective tuning of M/T cells to odorant molecules occurs in the OB. This phenomenon may be related to special features of olfactory circuitry. The odorants interact with olfactory sensory neurons (OSNs) and trigger the action potentials of OSNs with a specific olfactory receptor (OR) subtype which transmit to the OB. OSNs which express the same olfactory receptor gene converge their axons into the same glomerulus in the OB. This precise projection structure has led to discussion of molecular receptive ranges (Luo and Katz, 2001). Large odorant panels were applied to test the selective tuning of M/T cells. Imaging techniques allow in vivo visualization of glomeruli. Recent

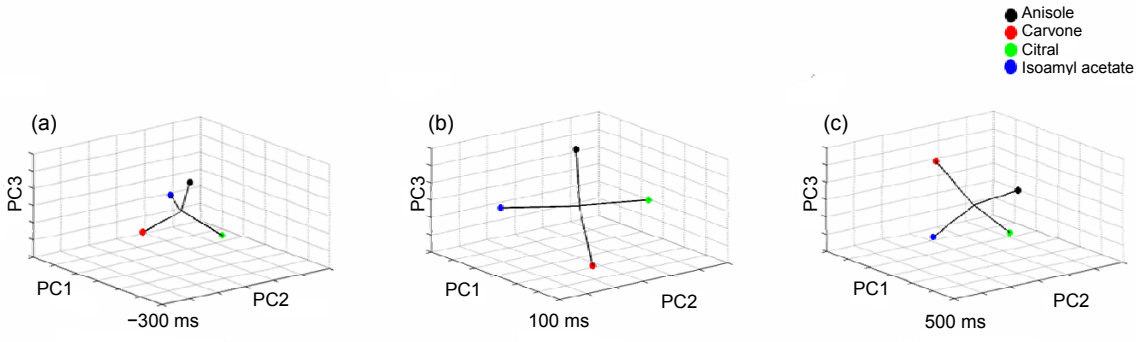

Fig. 4 Distribution of cell ensemble vectors in featured space
(a) 300 ms before odor onset; (b) 100 ms after odor onset; (c) 500 ms after odor onset

studies indicate that odorant identities are spatially mapped onto the glomerular layer (Rubin and Katz, 1999; Davison and Katz, 2007). The receptive ranges of M/T cells are highly restricted within chemical space. Therefore, single M/T cells were more responsive to one odor than to two or even three. The statistics of responsive cells showed that carvone most commonly elicited an odor-evoked response followed by citral, anisole, and isoamyl acetate. This may be related to the chemical structures of the odors and the molecular receptive ranges.

The breath of mammals provides rhythmical sampling from the outside environment. Exposing mammals to odors for a period of time showed that the firing of M/T cells was modulated by the respiration cycle (Chaput *et al*., 1992). During our recording, the breath signal of the rat was recorded by a piezoelectric belt around the rat's chest. Olfactory processing was believed to occur rapidly. However, the speed and accuracy of olfactory discrimination is still under discussion. One sniff has been shown to be enough for odor perception from the active sniff of a behaving rat (Uchida and Mainen, 2003). In our study in which, unlike previous studies, we provided a short-term odor stimulus. We also found that the response pattern of M/T cells showed rapid odor recognition during passive breathing. Under a puff stimulus, a distinct modified discharge from cells occurred within a short respiration cycle. Single cells were not widely responsive to all odorants and gave monotonic responses to odors. Thus, we pooled all recorded excitatory and inhibitory cells together, categorized by odor stimuli, assuming that the response variations of cells were acceptable among individuals. To uncover the temporal odor response of M/T cells, cell discharges were aligned to the initial phase of the inhalation after odor onset. The average firing rates evoked by the four odor stimuli were investigated (Fig. 2d). Within the first breathing cycle, a synchronous increase or decrease in firing rates was observed under all of the applied odor stimuli. The transient temporal responses indicated the odor perception happened quickly, like a 'snapshot'. The durations of the transient change were almost the same among the four odor stimuli. This synchronization phenomenon of unitary activities could be attributed to the common afferent input from glomeruli. M/T cells receive granular-induced inhibition with similar latencies and durations with a probability much higher than that of independent cells (Buonviso *et al*., 1996). The peaks or valleys of cell ensemble firing rate showed differences in frequency during odor stimuli. How are these changes presented to higher brain regions in terms of odor coding? The ensemble dynamics may reveal the response profiles involved in odor coding.

To represent ensemble activity from the resting state to the odor-evoked state, we used the population vector paradigm. Analyzed spike trains were selected over a time period of one breathing cycle pre-stimulation and two breathing cycles post-stimulation, a total of 1800 ms. The temporal activity of responsive cells is shown in Figs. 3c and 3d (upper panel). Cells of the same responsive pattern to one odor stimulus formed a multidimensional vector. Multidimensional vectors were constructed in which each dimension contained the instantaneous firing rate of a given cell accumulated over 100 ms bins. PC analysis was used to uncover odor response features in low dimension from high-dimensional data. Taking carvone excitatory cells for example, the activity of 84 cells was organized in 84-dimensional vectors and was decomposed into the first three PCs. The successive points in the three-dimensional (3D) space represent the temporal evolution of population activity in response to the stimulus. When points were connected in temporal order, the red segments of the trajectory represented the epoch during the first breathing cycle after odor stimulus while the black segments represented resting state activity. Figs. 3c and 3d provide a pictorial representation of population activities in response to the four odors. The trajectories were averaged over five trials (Fig. 3b). Each trial was calculated using the population vector constructed from the same cell ensemble exposed to the same odor at different times. Fig. 3c (lower panel) shows population information of excitatory cells in response to the four odors in 3D space, which reduced the dimension space of the vectors (original dimension space: carvone 84D, isoamyl acetate 73D, citral 79D, and anisole 72D). Fig. 3d (lower panel) shows population information of inhibitory cells in response to the four odors in 3D space (original dimension space: carvone 30D, isoamyl acetate 26D, citral 32D, and anisole 32D). These plots should be read as qualitative indices of M/T cell ensemble states.

The trajectories suggested that odor-evoked patterns move progressively further away from the resting state. The ensemble tracks leaving and returning to a noisy baseline state cost almost the same time among different trials, indicating that the response segment was modulated by respiration rather than being correlated with odor types. Excitatory trajectories appeared to take a longer distance to return to the resting state than inhibitory trajectories within the breathing cycle. Interestingly, the velocity of the stimulus-dependent segment tracking in the orbit had the same order in both excitatory and inhibitory patterns. The velocity of isoamyl acetate's trajectory (excitatory (*E*): (138.5±7.2) s^{-1}, n=5; inhibitory (*I*): (53.3±3.1) s^{-1}, n=5) within the breathing cycle was significantly faster than those of the other odors (p<0.05, one-way ANOVA test). The velocities of carvone (*E*: (121.4±8.5) s^{-1}, n=5; *I*: (41.6±4.1) s^{-1}, n=5), anisole (*E*: (109.4±7.6) s^{-1}, n=5; *I*: (36.2±6.2) s^{-1}, n=5), and citral (*E*: (97±4.6) s^{-1}, n=5; *I*: (30.3±2.6) s^{-1}, n=5) were relatively slow and showed no statistically significant difference among them (p>0.05, one-way ANOVA test). The significance and basis of the velocity difference need further investigation. The instantaneous velocity of mean odor trajectories during the first breathing cycle was faster than that in the resting state ((10.3±4.2) s^{-1}, n=40, p<0.05, one-way ANOVA test). The dynamic changes represent rapid odor perception.

The typical olfactory track consists of the receptor, glomerulus, principal neuron, and finally the brain. The general odor picture is very complex from level to level. Most previous studies have overlooked the function of inhibitory cells in odor information encoding (Stopfer, 2005). During the rapid process of odor perception, the trajectory of inhibitory cells also shows strong dynamics. This result indicates that odor pictures projected to the brain consist of spatiotemporal firing patterns of excitatory and inhibitory M/T cell ensembles within the first breathing cycle. To explore odor discrimination based on this idea, the vectors of cell ensemble responses to the four odors, involving both patterns, were constructed in the same space. Fig. 4 depicts the relative position of the cell ensemble before, at the onset of and after odor supply in three time slices. The distances from the cluster center of vectors to the origin enlarged during stimulation. After sensory processing in the olfactory system, the breadth of clusters shortened. This provides evidence that odor discrimination can be achieved by the representation of cell ensemble dynamics.

4 Conclusions

Recent studies have discussed the suggestion that odor information is transmitted on a fast timescale. Inspired by the idea that active sniffing induces a quick odor-evoked response, we propose that passive breathing also has rapid odor perception under short-term odor stimulation. In the present study, we investigated the responses of M/T cell ensembles to four pure chemicals using anesthetized freely breathing rats and a multielectrode array. Each pure chemical with different functional groups differed from each other incrementally. The M/T cells selectively responded to the odors with excitation or inhibition patterns. We showed featured odor trajectories of cell ensembles extracted from temporal cell firings. Stimulated by a short time odor puff, the obvious changing track indicated that odor information encodings were completed within a single respiration cycle. Furthermore, we observed the breadth of clusters enlarged in feature space during stimulation. This supported our finding that odor discrimination in the olfactory bulb happens within the first breathing cycle.

Acknowledgements

We thank Prof. Xiao-xiang ZHENG from Department of Biomedical Engineering, Zhejiang University, China for her kind discussion.

References

Bathellier, B., van de Ville, D., Blu, T., Unser, M., Carleton, A., 2007. Wavelet-based multi-resolution statistics for optical imaging signals: application to automated detection of odour activated glomeruli in the mouse olfactory bulb. *Neuroimage*, **34**(3):1020-1035. [doi:10.1016/j.neuroimage.2006.10.038]

Bathellier, B., Buhl, D.L., Accolla, R., Carleton, A., 2008. Dynamic ensemble odor coding in the mammalian olfactory bulb: sensory information at different timescales. *Neuron*, **57**(4):586-598. [doi:10.1016/j.neuron.2008.02.011]

Buonviso, N., Chaput, M.A., Berthommier, F., 1996. Similarity of granular-induced inhibitory periods in pairs of neighboring mitral/tufted cells. *J. Neurophysiol*., **76**(4):2393-2401.

Buonviso, N., Amat, C., Litaudon, P., Roux, S., Royet, J.P., Farget, V., Sicard, G., 2003. Rhythm sequence through the olfactory bulb layers during the time window of a respiratory cycle. *Eur. J. Neurosci*., **17**(9):1811-1819. [doi:10.1046/j.1460-9568.2003.02619.x]

Chaput, M.A., 1986. Respiratory-phase-related coding of olfactory information in the olfactory bulb of awake freely-breathing rabbits. *Physiol. Behav*., **36**(2):319-324. [doi:10.1016/0031-9384(86)90023-5]

Chaput, M.A., Buonviso, N., Berthommier, F., 1992. Temporal patterns in spontaneous and odour-evoked mitral cell discharges recorded in anaesthetized freely breathing animals. *Eur. J. Neurosci*., **4**(9):813-822. [doi:10.1111/j.1460-9568.1992.tb00191.x]

Chen, T.W., Lin, B.J., Schild, D., 2009. Odor coding by modules of coherent mitral/tufted cells in the vertebrate olfactory bulb. *PNAS*, **106**(7):2401-2406. [doi:10.1073/pnas.0810151106]

Couto, A., Alenius, M., Dickson, B.J., 2005. Molecular, anatomical, and functional organization of the drosophila olfactory system. *Curr. Biol*., **15**(17):1535-1547. [doi:10.1016/j.cub.2005.07.034]

Cury, K.M., Uchida, N., 2010. Robust odor coding via inhalation-coupled transient activity in the mammalian olfactory bulb. *Neuron*, **68**(3):570-585. [doi:10.1016/j.neuron.2010.09.040]

Davison, I.G., Katz, L.C., 2007. Sparse and selective odor coding by mitral/tufted neurons in the main olfactory bulb. *J. Neurosci*., **27**(8):2091-2101. [doi:10.1523/Jneurosci.3779-06.2007]

Egana, J.I., Aylwin, M.L., Maldonado, P.E., 2005. Odor response properties of neighboring mitral/tufted cells in the rat olfactory bulb. *Neuroscence*, **134**(3):1069-1080. [doi:10.1016/j.neuroscience.2005.04.027]

Feinstein, P., Mombaerts, P., 2004. A contextual model for axonal sorting into glomeruli in the mouse olfactory system. *Cell*, **117**(6):817-831. [doi:10.1016/j.cell.2004.05.011]

Friedrich, R.W., Laurent, G., 2001. Dynamic optimization of odor representations by slow temporal patterning of mitral cell activity. *Science*, **291**(5505):889-894. [doi:10.1126/science.291.5505.889]

Isaacson, J.S., Cang, J.H., 2003. In vivo whole-cell recording of odor-evoked synaptic transmission in the rat olfactory bulb. *J. Neurosci*., **23**(10):4108-4116.

Kay, L.M., Laurent, G., 1999. Odor- and context-dependent modulation of mitral cell activity in behaving rats. *Nat. Neurosci*., **2**(11):1003-1009.

Laing, D.G., 1986. Identification of single dissimilar odors is achieved by humans with a single sniff. *Physiol. Behav*., **37**(1):163-170. [doi:10.1016/0031-9384(86)90400-2]

Leon, M., Johnson, B.A., 2003. Olfactory coding in the mammalian olfactory bulb. *Brain Res. Rev*., **42**(1):23-32. [doi:10.1016/s0165-0173(03)00142-5]

Luo, M.M., Katz, L.C., 2001. Response correlation maps of neurons in the mammalian olfactory bulb. *Neuron*, **32**(6):1165-1179. [doi:10.1016/s0896-6273(01)00537-2]

Meister, M., Bonhoeffer, T., 2001. Tuning and topography in an odor map on the rat olfactory bulb. *J. Neurosci*., **21**(4):1351-1360.

Mombaerts, P., 1996. Targeting olfaction. *Curr. Opin. Neurobiol*., **6**(4):481-486. [doi:10.1016/S0959-4388(96)80053-5]

Restrepo, D., Doucette, W., Whitesell, J.D., Mctavish, T.S., Salcedo, E., 2009. From the top down: Flexible reading of a fragmented odor map. *Trends Neurosci*., **32**(10):525-531. [doi:10.1016/j.tins.2009.06.001]

Rinberg, D., Koulakov, A., Gelperin, A., 2006. Sparse odor coding in awake behaving mice. *J. Neurosci*., **26**(34):8857-8865. [doi:10.1523/Jneurosci.0884-06.2006]

Rubin, B.D., Katz, L.C., 1999. Optical imaging of odorant representations in the mammalian olfactory bulb. *Neuron*, **23**(3):499-511.

Stopfer, M., 2005. Olfactory coding: inhibition reshapes odor responses. *Curr. Biol*., **15**(24):R996-R998. [doi:10.1016/j.cub.2005.11.052]

Uchida, N., Mainen, Z.F., 2003. Speed and accuracy of olfactory discrimination in the rat. *Nat. Neurosci*., **6**(11):1224-1229. [doi:10.1038/nn1142]

Wellis, D.P., Scott, J.W., Harrison, T.A., 1989. Discrimination among odorants by single neurons of the rat olfactory bulb. *J. Neurophysiol*., **61**(6):1161-1177.

Wilson, R.I., Mainen, Z.F., 2006. Early events in olfactory processing. *Annu. Rev. Neurosci*., **29**:163-201. [doi:10.1146/annurev.neuro.29.051605.112950]